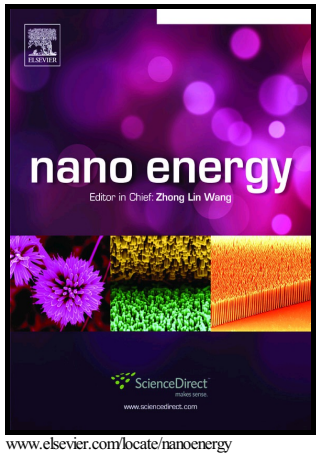

www.elsevier.com/locate/nanoenergy

Flexible thermoelectric foil for wearable energy harvesting

Chunlei Wan, Ruoming Tian, Azrina Binti Azizi, Yujia Huang, Qingshuo Wei, Ryo Sasai, Soontornchaiyakul Wasusate, Takao Ishida, Kunihito Koumoto

PII: S2211-2855(16)30374-3
DOI: http://dx.doi.org/10.1016/j.nanoen.2016.09.011
Reference: NANOEN1490

To appear in: *Nano Energy*

Received date: 5 July 2016
Revised date: 26 August 2016
Accepted date: 7 September 2016

Cite this article as: Chunlei Wan, Ruoming Tian, Azrina Binti Azizi, Yujia Huang, Qingshuo Wei, Ryo Sasai, Soontornchaiyakul Wasusate, Takao Ishida and Kunihito Koumoto, Flexible thermoelectric foil for wearable energy harvesting, *Nano Energy,* http://dx.doi.org/10.1016/j.nanoen.2016.09.011

Flexible thermoelectric foil for wearable energy harvesting

Chunlei Wan[1,*], Ruoming Tian[2], Azrina Binti Azizi[3], Yujia Huang[1], Qingshuo Wei[4], Ryo Sasai[5], Soontornchaiyakul Wasusate[5], Takao Ishida[4], Kunihito Koumoto[2,*]

[1]*State Key Laboratory of New Ceramics and Fine Processing, School of Materials Science and Engineering, Tsinghua University, Beijing 100084, China*

[2]*Toyota Physical and Chemical Research Institute, Nagakute 480-1192, Japan*

[3]*Graduate School of Engineering, Nagoya University, Nagoya 464-8603, Japan*

[4]*Nanosystem Research Institute, National Institute of Advanced Industrial Science and Technology, 1-2-1 Namiki, Tsukuba, Ibaraki 305-8564, Japan*

[5]*Interdisciplinary Graduate School of Science and Engineering, Shimane University, 1060 Nishikawatsu-cho, Matsue 690-8504, Japan*

wancl@mail.tsinghua.edu.cn

koumoto@toyotariken.jp

[*]Corresponding authors.

Abstract

Flexible thermoelectric (TE) devices have been of rapidly growing interest for long-lasting and maintenance-free wearable power source that makes use of the temperature difference between human skin and ambient environment. Despite the high TE performance, conventional inorganic TE semiconductors, such as Bi_2Te_3, skutterudies, are restricted for this application due to their non-flexibility structure and non-scalable manufacturing techniques. In this paper, we report large-area free-standing TE foil with several centimeters in size through a scalable, cost-effective and solution-based approach for flexible thermoelectric devices. The foil is made by self-assembling two-dimensional hybrid superlattices of TiS_2 layers and hexylammine molecules. Through a Lewis base-acid reaction, electrons are transferred from the hexylamine molecules into the TiS_2 layers, making the material

n-type and generating a large power factor of 0.23 mW/mK^2, comparable to the best p-type conducting polymers. The flexible foil shows superior bending deformation tolerance, even better than the conducting polymers. A power output of 32 μWcm^{-2} for a 15-μm-thick foil were obtained under a temperature difference of 20K at ambient temperature, high enough to drive the wearable nanowatt-to-microwatt level circuit chips or devices.

Keywords: flexible, thermoelectric, wearable, intercalation, transitional metal dichalcogenide

1. Introduction

Flexible thermoelectric (TE) materials and devices have attracted increasing attentions recently, especially in the field of wearable electronics.[1, 2, 3, 4] By converting heat energy of human body into electricity, flexible TE generator can provide long-lasting and reliable power supply for those explosively developing flexible electronic devices. Compared with the currently used batteries that need frequent recharging and replacement, TE generator almost needs no maintenance or users' intervention and thereby possesses great advantages. On the other hand, wearable flexible thermoelectric modules can heat or cool human body by Peltier effect, thereby enabling smart personal thermal management. In this way, large amount of energy that are wasted on heating or cooling the empty space or inanimate object inside buildings can be saved.[5]

The major challenge for the flexible TE module is to fabricate cost-effective TE materials that show excellent mechanical flexibility, good thermoelectric performance and possibility of large-area productions through solution-based printing process. Conventional thermoelectric materials, such as Bi_2Te_3 and PbTe, and recently developed state-of-the-art materials, such as skutterudites, clathrates, silicides, etc.,[6] all show high TE performance, but they are all inorganic materials and intrinsically rigid. Screen printing method was used to make inorganic films on a soft substrate, into which microspores were introduced to achieve a certain degree of flexibility.[2, 7, 8] However, the flexibility is quite limited: the lowest bending radius of the film is around 30 mm, which severely restricts its surface conformability and application in wearable electronics.[8] Furthermore, the porosity leads to a huge degradation of thermoelectric performance compared with their bulk counterpart.

Organic conducting polymers could be an ideal option for flexible thermoelectrics. P-type PEDOT:PSS with optimized carrier concentration and microstructure, has been proved to possess both excellent flexibility and high TE performance together with versatile processability.[9, 10, 11, 12] However, there is a big issue to overcome for conducting polymers, the lack of n-type organic TE materials to make p-n couples for TE modules. Owing to the low affinity of organic materials, there remains a challenge for n-doped polymers to increase their conductivity while maintain air stability.[13] Accordingly, a high performance air-stable n-type counterpart is strongly required to make p-n couples for thermoelectric modules in order to realize high-power generators.

In this paper, we report an n-type flexible thermoelectric material by simply grinding a transitional metal dichalcogenide TiS_2 and a Lewis base hexylamine molecules using a mortar and pestle. The empty 3*d* orbital of the Ti atoms can accept electrons from the hexylamine molecules through a Lewis acid-base reaction, making the material n-type. Meanwhile, the organic molecules are intercalated into the van der Waals gap between the TiS_2 layers and the hybrid material becomes flexible due to the layer expansion. A salable solution-based self-assembling technique is developed to make large-area flexible foil based on these hybrid inorganic/organic superlattices, which shows great potential for practical manufacturing of flexible thermoelectric devices.

2. Experimental section

The hybrid $TiS_2HA_xNMF_y$ foil was synthesized by a simple liquid exfoliation method followed by a self-assembly process. Firstly, TiS_2 powder was synthesized by sealing stoichiometric Ti and Sulfur powder in evacuated silica tube and heated at 600 ^oC for one week. Then, 0.2g TiS_2 powder was thoroughly mixed and ground with hexylamine (99.0%, Tokyo Chemical Industry) with a molar ratio of 1:4. The resultant powder showed a metallic brown color. The mixed powder was then transferred into a glass veil with 45ml N-methylformamide (99.0%, Tokyo Chemical Industry). The veil was placed in a sonic bath (Branson 2510J-DTH) for 1 h, which resulted in navy dispersion. The obtained dispersion was then centrifuged. The supernatant was removed to a petri dish and dried in a vacuum oven at 130^oC.

The foil was characterized by XRD, and X-ray photoemission spectroscopy. To quantitatively analyze the composition of the $TiS_2HA_xNMF_y$ foil, it was pulverized and ultrasonically dispersed in D_2O and then sealed in a glass tube followed by heating at 180^oC for 1 h. The intercalated organic molecules were then evaporated into D_2O and the composition of the foil was measured by nuclear magnetic resonance. Polarized FTIR was used to determine the orientation of the hexylammonium molecules. The cross-sections of the samples were observed by SEM. The surface roughness was measured by 3D confocal laser microscope (Olympus).

The elastic properties were measure by Thermo-Mechanical Analyzer (Netzsch TMA 402). The hall measurement was performed on a commercial system (TOYO Corporation, ResiTest8300). The in-plane Seebeck coefficient, electrical conductivity were measured using a home-made system.[14] The in-plane thermal diffusivity of the hybrid foil was measured by a special thermal wave method using the Ai-Phase system (Hitachi), for which the foil was sliced and arrayed in a parallel way. The heat capacity was measured by the differential scanning calorimetry (DSC) method. The in-plane thermal conductivity was then calculated as a product of the thermal diffusivity, heat capacity and density. The flexibility was tested by pressing the foil onto glass tubes with different radii and the resistance was measured by van der Pauw method.

3. Results and discussion

TiS_2-based inorganic/organic superlattice was previously fabricated by an electrochemical intercalation method, where TiS_2 single crystal with a typical size of 4mm x 4mm x 100 μm was set as a cathode.[14] Organic cations dissolved in the electrolytes were intercalated into the van der Waals gap of the TiS_2 single crystals under the electrostatic force, forming a TiS_2/organic hybrid superlattice. The final product of this method is limited by the pristine TiS_2 single crystal which is very difficult to grow into large sizes for mass production.

Here we report a facile solution-based method to fabricate scalable flexible foils with the inorganic/organic superlattice structure, as shown in Fig. 1 and Supplementary Fig. 1. TiS_2 powder was mechanically ground with hexylamine (HA; $C_6H_{13}NH_2$) liquid. During the mixing process, TiS_2 gradually react with the organic molecules, as TiS_2 has empty Ti 3d orbitals and can accept electrons from HA molecules which behave as a Lewis base (electron donor) due to the presence of the lone pair electrons in the nitrogen atom.[15] Electrons were thus transferred from the HA molecules to TiS_2, leaving TiS_2 negatively charged with partially reduced Ti^{3+} and HA molecules positively ionized.[16] Meanwhile, the resultant organic cations (HA^+) are intercalated into the van der Waals gap of TiS_2 by the electrostatic force simultaneously.[16, 17]

After grinding for 30 minutes, the liquid HA gradually disappears and the volume of the powder expands, indicating that HA molecules are intercalated into TiS_2 particles. The X-ray diffraction shows that the c-axis lattice constant significantly increased by 4 times compared with the pristine TiS_2 corresponding to the interlayer

distance of 2.23 nm (Fig. 2a), which coincides with the swelling of the sample observed after mixing. The interlayer distance expansion (1.66 nm) is slightly smaller than twice of the length of a HA molecule (1.04 nm), which would indicate HA molecules form paraffin-like bilayer structure with a certain degree of inclination in the van der Waals gap of TiS_2.[18]

The as-prepared powder is then immersed into a highly polarized organic solvent, N-methylformamide (NMF; C_2H_5NO). As HA molecules are already partially ionized, the polar organic solvents could be easily incorporated into the van der Waals gap by the cation-dipole interactions.[19] As NMF has very high dielectric constant, the cation-dipole interactions are strong enough and can further expand the interlayer distance of the TiS_2 layers, resulting in weakening the interlayer forces. Then, by vigorous ultrasonication the $TiS_2HA_xNMF_y$ layers become exfoliated into nanosheets. The AFM image shows that typical nanosheets are about several hundred nanometers in lateral width and about 2 nanometers in thickness. (Fig. 2b)

A TEM image of the planar surface of the TiS_2/organic nanosheet (Fig. 2c) coincides with the lattice structure of a pure TiS_2 crystal. The organic molecules cannot be seen in TEM in this direction due to its low scattering coefficient of electrons. The pattern of TiS_2 and one set of SAED pattern suggests that all the TiS_2 layers in this hybrid superlattice are stacked in an ordered way and there is no translational displacement or reorientation between the layers.

After the as-prepared liquid-solid mixture solution is centrifugally separated, the supernatant liquid is taken out to a petri dish and dried at 130^{o}C in a vacuum oven.

After 3 hours, the solvent is evaporated and the $TiS_2HA_xNMF_y$ nanosheets are deposited onto the bottom surface of the petri dish and a large-area foil is formed by self-assembly. As the nanosheets are highly anistotropic, the forces exerted by surface tension with the evaporation of solvent can easily cause well alignment of the lamella onto the flat surface of the petri dish. Therefore, flat and highly coherent films can be obtained. Depending on the size of the petri dish, the area of the foil could be up to tens of centimeter. The thickness ranges from several to a few hundred micrometer, depending on the volume of the supernatant. It is important to point out that this approach will enable the fabrication of large area devices by solution processing. This consideration is especially important when making organic p-n couples for thermoelectric modules.

To quantitatively analyze the composition of the $TiS_2HA_xNMF_y$ foil, it was pulverized and ultrasonically dispersed in D_2O and then sealed in a glass tube followed by heating at 180^oC for 1 h. The intercalated organic molecules were then evaporated into D_2O and the composition of the foil was measured by nuclear magnetic resonance (^{1}H-NMR) analysis to be $TiS_2HA_{0.01}NMF_{0.003}$. (See the supplementary Fig. 2.)

Nanostructure of the as-prepared $TiS_2HA_{0.01}NMF_{0.03}$ foil was then further characterized. The XRD patterns are shown in Fig. 2a. Compared with the pristine TiS_2, the (00ℓ) peaks systematically move to the lower diffraction angles, indicating an expansion of the lattice along the c-axis. Using the Bragg equation, the lattice constant, *c*, was calculated to be 1.02 nm, which is larger than that of the pristine TiS_2

(0.569 nm), but is much smaller than that of the TiS_2/HA after the first mixing (2.23 nm). This must be due partly to the different composition and partly to a possible rearrangement of HA molecules in the van der Waals gap. In order to analyze the arrangement of HA molecules, polarized FT-IR spectroscopy was employed for the nanosheets deposited onto a CaF_2 substrate (Supplementary Fig. 3). The result shows that the chain axis of the HA molecule lies parallel to the basal plane of the [TiS_2] layer. Combining the chemical composition, XRD, and FT-IR information and considering the size of each molecule (HA: l=1.044 nm and w=0.178 nm; NMF: l= 0.413 nm and w= 0.231 nm) and the thickness of a [TiS_2] monolayer (0.279 nm), it can be estimated that a layer composed of [10HA−3NMF] mainly consists of the organic layer in the van der Waals gap of TiS_2.

As shown in Fig. 2d, e, the surface roughness of the as-prepared foil observed with a 3D laser microscope is about 155 nm, suggesting the surface is not so smooth though it shows metallic color. The cross section of the foil were observed by SEM (Fig. 2f, g). It shows that the thickness is about 15 μm. It shows that all the nanosheets are well aligned with some degree of distortion, showing a wavy-like structure.

Thermoelectric properties of the TiS_2 hybrid foil are shown in Fig. 3. The properties of a TiS_2 single crystal are also included for comparison. The electrical conductivity of the TiS_2 foil is much higher than that of the TiS_2 single crystal in the in-plane direction. The electrical conductivity is determined by two factors, *id est.* carrier concentration and mobility. TiS_2 is a narrow band-gap semiconductor, and during synthesis process, a small amount of excess Ti atoms easily become

self-intercalated into the van der Waals gap, donating electrons into the conduction band.[20] When forming $TiS_2HA_xNMF_y$ hybrid, lone-pair electrons are transferred from the nitrogen atoms of HA to the 3d orbitals of the Ti atoms, resulting in further increase in carrier concentration, which can account for the increase in the electrical conductivity. In fact, Hall measurements show that the carrier concentration of the TiS_2 foil ($1.35x10^{21}$ cm^{-3}) is much larger than that of the TiS_2 single crystal ($1.76x10^{20}$ cm^{-3}). If one nitrogen atom of a HA molecule donates one electron to a [TiS_2] layer, the carrier concentration is estimated to become ~$2.8x10^{20}$ cm^{-3} according to the chemical formula, $TiS_2HA_{0.01}NMF_{0.003}$, which is much less than the measured carrier concentration. This discrepancy may be explained that during the heating process, most HA^+ ions were evaporated in the form of neutral HA molecules but left H^+ bonded with TiS_2 layers and compensated the negative charges[21]. The increase of carrier concentration would indicate the increase in Ti^{3+} concentration, which was verified by the XPS analysis showing that some peaks corresponding to Ti^{3+} appeared after intercalation (Fig. 3c). The mobility of the $TiS_2HA_{0.01}NMF_{0.003}$ foil was measured to be 2.4 $cm^2V^{-1}s^{-1}$, which is degraded compared with that of TiS_2 single crystal (7.2 $cm^2V^{-1}s^{-1}$). As the foil is composed of multiple nanosheets, where electrons jumping across the nanosheets are scattered by the nanosheet-to-nanosheet interfaces, resulting in an increase in the electrical resistance and hence a decrease in mobility. Although the mobility slightly decreased, the electrical conductivity was enhanced due to the increase in carrier concentration reaching about 520 S/cm at room temperature.

As a result of the increased carrier concentration, the Seebeck coefficient of the TiS_2 hybrid foil is lower than that of the TiS_2 single crystal. The power factor of the TiS_2 hybrid foil is 0.23 $mWm^{-1}K^{-2}$ at 300K which is much reduced compared with the TiS_2 single crystal (1.15 $mWm^{-1}K^{-2}$). However, it is among the highest values for the flexible n-type thermoelectric materials.[1] It is almost comparable to the best p-type conducting polymers, such as PEDOT:PSS (0.469 $mWm^{-1}K^{-2}$) and carbon nanotube network (0.34 $mWm^{-1}K^{-2}$)[22]. It is even higher than that of a flexible inorganic Bi_2Te_3 thin film (0.18 mWm^{-1} K^{-2}) where the porous structure was introduced to increase the flexibility but severely deteriorated the electrical conductivity[7].

As shown in Fig. 3e, the in-plane thermal conductivity of a TiS_2 hybrid foil was 6~7 times lower than that of the TiS_2 single crystal. Using the Wiedemann-Franz law, the in-plane lattice thermal conductivity of the hybrid foil was calculated to be 0.43 W/mK at room temperature, one order of magnitude lower than that of TiS_2 single crystal, 4.2 W/mK. Molecular dynamics simulation[14] on thermal conductivity of the hybrid material has suggested that all the acoustic phonon branches were broadened, indicating that the acoustic phonons transporting inside the layers were remarkably damped by the organic molecules that are chemically bonded to the TiS_2 layers. Another reason for the low thermal conductivity is that the interface between the neighboring nanosheets could further scatter the phonons.

Though the power factor of the hybrid material is much lower, the *ZT* value is improved compared with that of the TiS_2 single crystal owing to the great reduction in thermal conductivity. At 393K, a *ZT* value of 0.12 was obtained. Though it is still low

compared with those of state-of-the-art Bi_2Te_3-based materials, it is useful in some situations where the *ZT* value is not the primary concern. Especially, both mechanical flexibility and high-power output are much more important for wearable electronics.

The foil becomes very soft and the elastic properties were fully characterized. As shown in Fig. 4a, a typical stress-strain curve of the foil shows three regimens of deformation before failure: (I) straightening, (II) elongation and (III) plastic deformation. In regime I, as the foil has a distorted wavy-like microstructure (Fig. 2), the layers have to be straightened first, which would need a smaller stress. Modules of this regime is calculated to be 21 MPa. The second regime may correspond to the in-plane lattice stretching of the $TiS_2HA_{0.01}NMF_{0.003}$ (mainly the TiS_2 layers) and shows a higher tensile modulus (250 MPa), as it is determined by the intrinsic covalent bonding of the Ti-S network. The third plastic regime, the nanosheets inside the foil may have slipped under the tensile stress before failure. The tensile strength of the foil is 8.0 MPa, which is larger than that of typical commercial graphite foils (4.0MPa~5.2MPa).[23] Though the Ti-S bonding in a TiS_2 foil is much weaker than the C-C bonding in a graphite foil, a TiS_2 foil shows higher tensile strength due to the strong bonding between the assembled nanosheets. The bending modulus of the $TiS_2HA_{0.01}NMF_{0.003}$ foil is measured to be1.59 GPa, which is higher than that of a single crystalline plate of $TiS_2HA_{0.08}H_2O_{0.22}DMSO_{0.03}$, likely because the $TiS_2HA_{0.01}NMF_{0.003}$ foil has much less organic molecules. [14]

To test the flexibility of the foil, it was bent to different radii and the electrical resistance was measured as a function of the bending radius (Fig. 4b). The electrical

resistance remains almost unchanged even the foil is bent to a radii of 3 mm, which is one order of magnitude larger than the screen-printed Bi_2Te_3 film.[8] It is even better than the conducting polymer, PEDOT:PSS, which shows an abrupt increase of electrical resistance when the bending radius is lower than 5 mm.[24] This is mainly due to the intrinsically flexible structure of the foil. The original TiS_2 single crystal is rigid, in which [TiS_2] layers are connected by van der Waals force, but by intercalating organic molecules into the gap the interlayer distance is enlarged, and the resulting soft and flexible microstructure can tolerate large deformation without severely deteriorating the electronic conduction path. Accordingly, this result would indicate that the electrical resistance is almost unaffected when the foil is attached to a non-flat surface, which is very important for flexible devices.

To test the power generation characteristics of the flexible foil, a simple single-leg device was made, as shown in the inset picture of Fig. 4c. A piece of freestanding foil of 5mm (L)*5mm (W)*15μm (T) was placed on the top of two reverse Peltier modules. The temperature difference across the foil was controlled by the current through the Peltier modules. It shows that under a temperature difference of 20 K generated a maximum power output of 24 nW and a power density of 32 μW/cm^2. It is enough to drive those nanowatt-level circuit chips[25, 26]. Furthermore, the output power level can be expected to boost up to microwatt with the size of the foil, such as multilayers with larger area, thereby being able to drive the low-power wearable electronic electronics, such as sensor, wireless communication, signals amplifying and sophisticated signal processing.[27, 28]

4. Conclusions

In summary, we report an n-type free-standing flexible thermoelectric foil by assembling two-dimensional nanosheets of hybrid TiS_2/hexylamine superlattices. The foil is extremely soft and can undertake sever bending deformation without deteriorating the properties. A large power factor of 0.23 mW/mK^2 at room temperature was obtained, which is among the best flexible n-type thermoelectric materials. This low-cost, large-area, robust, solution-processable, light-weight and nontoxic flexible thermoelectric foil shows great potential for wearable power source that makes use of heat energy of human body, or personal temperature management by peltier effect. In addition, the fabrication process can be a general route to make freestanding foils of other two dimensional materials, such as TaS_2, VS_2, MoS_2, CrS_2, NbS_2, VS_2, etc. to make new foil with potentially higher TE properties or other functional properties.

Acknowledgements

C.W. acknowledges financial support from 1000 Plan Program for Young Talents of China. K. Koumoto acknowledges financial support from JSPS KAKENHI grant no. 25289226 and NEDO-TherMat.

References

1. Bahk J-H, Fang H, Yazawa K, Shakouri A. Flexible thermoelectric materials and device optimization for wearable energy harvesting. *Journal of Materials Chemistry C* 2015, **3**(40)**:** 10362-10374.

2. Yadav A, Pipe KP, Shtein M. Fiber-based flexible thermoelectric power generator. *Journal of Power Sources* 2008, **175**(2)**:** 909-913.
3. Sevilla GAT, Bin Inayat S, Rojas JP, Hussain AM, Hussain MM. Flexible and Semi-Transparent Thermoelectric Energy Harvesters from Low Cost Bulk Silicon (100). *Small* 2013, **9**(23)**:** 3916-3921.
4. Dun C, Hewitt CA, Huang H, Xu J, Montgomery DS, Nie W, *et al.* Layered Bi2Se3 Nanoplate/Polyvinylidene Fluoride Composite Based n-type Thermoelectric Fabrics. *Acs Applied Materials & Interfaces* 2015, **7**(13)**:** 7054-7059.
5. Hsu P-C, Liu X, Liu C, Xie X, Lee HR, Welch AJ, *et al.* Personal Thermal Management by Metallic Nanowire-Coated Textile. *Nano Letters* 2015, **15**(1)**:** 365-371.
6. Snyder GJ, Toberer ES. Complex thermoelectric materials. *Nature Materials* 2008, **7**(2)**:** 105-114.
7. Lu ZY, Layani M, Zhao XX, Tan LP, Sun T, Fan SF, *et al.* Fabrication of Flexible Thermoelectric Thin Film Devices by Inkjet Printing. *Small* 2014, **10**(17)**:** 3551-3554.
8. We JH, Kim SJ, Cho BJ. Hybrid composite of screen-printed inorganic thermoelectric film and organic conducting polymer for flexible thermoelectric power generator. *Energy* 2014, **73:** 506-512.
9. Kim GH, Shao L, Zhang K, Pipe KP. Engineered doping of organic semiconductors for enhanced thermoelectric efficiency. *Nature Materials* 2013, **12**(8)**:** 719-723.
10. Chen Y, Zhao Y, Liang Z. Solution processed organic thermoelectrics: towards flexible thermoelectric modules. *Energy & Environmental Science* 2015, **8**(2)**:** 401-422.
11. Wei Q, Mukaida M, Naitoh Y, Ishida T. Morphological Change and Mobility Enhancement in PEDOT:PSS by Adding Co-solvents. *Advanced Materials* 2013, **25**(20)**:** 2831-2836.
12. Bubnova O, Khan ZU, Malti A, Braun S, Fahlman M, Berggren M, *et al.* Optimization of the thermoelectric figure of merit in the conducting polymer poly(3,4-ethylenedioxythiophene). *Nature Materials* 2011, **10**(6)**:** 429-433.
13. Crispin X. Carbon nanotubes get high. *Nature Energy* 2016, **1:** 16037.
14. Wan C, Gu X, Dang F, Itoh T, Wang Y, Sasaki H, *et al.* Flexible n-type thermoelectric materials by organic intercalation of layered transition metal dichalcogenide TiS_2. *Nature Materials* 2015, **14**(6)**:** 622-627.
15. Gamble FR, Osiecki JH, Cais M, Pisharod.R. INTERCALATION COMPLEXES OF LEWIS BASES AND LAYERED SULFIDES - LARGE CLASS OF NEW SUPERCONDUCTORS. *Science* 1971, **174**(4008)**:** 493-&.
16. Bernard L, McKelvy M, Glaunsinger W, Colombet P. EVIDENCE FOR AMMONIA OXIDATION AND THE IONIC NATURE OF AMMONIATED TITANIUM DISULFIDE. *Solid State Ionics* 1985, **15**(4)**:** 301-310.
17. Butz T, Saitovitch H, Lerf A, Zagefka HD, Schollhorn R. CHARGE-TRANSFER IN LAYERED COMPOUND TaS_2 INTERCALATED WITH NH_3 STUDIED BY PERTURBED ANGULAR-CORRELATIONS. *Phys Lett A* 1978, **67**(1)**:** 74-76.
18. Schollho.R, Weiss A. CATION-EXCHANGE REACTIONS AND LAYER SOLVATE COMPLEXES OF TERNARY PHASES M_XMoS_2. *Journal Of the Less-Common Metals* 1974, **36**(1-2)**:** 229-236.
19. Wan C, Kodama Y, Kondo M, Sasai R, Qian X, Gu X, *et al.* Dielectric Mismatch Mediates Carrier Mobility in Organic-Intercalated Layered TiS_2. *Nano Letters* 2015, **15**(10)**:** 6302-6308.

20. Kukkonen CA, Kaiser WJ, Logothetis EM, Blumenstock BJ, Schroeder PA, Faile SP, *et al.* TRANSPORT AND OPTICAL-PROPERTIES OF $TI_{1+X}S_2$. *Physical Review B* 1981, **24**(4)**:** 1691-1709.
21. Riekel C. KINETIC STUDY OF NH_3-ND_3 EXCHANGE IN TaS_2 BY NEUTRON-DIFFRACTION. *Solid State Communications* 1978, **28**(5)**:** 385-387.
22. Avery AD, Zhou BH, Lee J, Lee E, Miller EM, Ihly R, *et al.* Tailored semiconducting carbon nanotube networks with enhanced thermoelectric properties. *Nature Energy* 2016, **1:** 16033.
23. http://www.hpmsgraphite.com/graphitefoil.html.
24. Cho CK, Hwang WJ, Eun K, Choa SH, Na SI, Kim HK. Mechanical flexibility of transparent PEDOT:PSS electrodes prepared by gravure printing for flexible organic solar cells. *Sol Energy Mater Sol Cells* 2011, **95**(12)**:** 3269-3275.
25. http://ww1.microchip.com/downloads/en/DeviceDoc/30009941F.pdf
26. Morimura H, Oshima S, Matsunaga K, Shimamura T, Harada M. Ultra-low-power circuit techniques for mm-size wireless sensor nodes with energy harvesting, *IEICE Electron Expr* 2014, **11**(20): 1-12
27 http://cap.ee.ic.ac.uk/~pdm97/powermems/2012/oral/I-III.pdf
28 Chandrakasan AP, Verma N, Daly DC. Ultralow-Power electronics for biomedical applications, *Annu Rev Biomed* 2008, **10**:247-274

Figure 1 | A solution-based synthesis procedure of flexible $TiS_2HA_xNMF_y$ foil

Figure 2 | Structural Characterization of $TiS_2HA_xNMF_y$ nanosheet and foil. **(a)** XRD patterns of pristine TiS_2 powder and TiS_2 powder/Hexalmine mixture and $TiS_2HA_xNMF_y$ Foil. The (00*n*) peaks were observed, but only the 001 peaks were indexed for clarity. **(b)** AFM image of the $TiS_2HA_xNMF_y$ nanosheets after sonication. **(c)** HRTEM of $TiS_2HA_xNMF_y$ nanosheet. **(d)** Surface appearance of a $TiS_2HA_xNMF_y$ Foil. **(e)** Surface scanning of 2.5mm $\times$ 2.5mm area, showing that the surface roughness, R_a, is 155nm. **(f)**, **(g)** SEM images of the cross section of the foil.

Figure 3 | In-plane thermoelectric properties and XPS spectrum of the $TiS_2HA_{0.01}NMF_{0.003}$ foil compared with a TiS_2 single crystal. **(a)** electrical conductivity, **(b)** Seebeck coefficient, **(c)** XPS spectrum showing the presence of Ti^{3+} in the foil. **(d)** thermal conductivity, **(e)** power factor, **(f)** thermoelectric figure of merit,

ZT.

Figure 4 | (a) Stress-strain curve of a $TiS_2HA_{0.01}NMF_{0.003}$ foil. **(b)** Foil resistance change as a function of bending radius, where R_0 and R is the foil resistance before and after bending. **(c)** Current-voltage and power curve for a flexible $TiS_2HA_{0.01}NMF_{0.003}$ foil under a temperature difference of 35K.

Figure 1

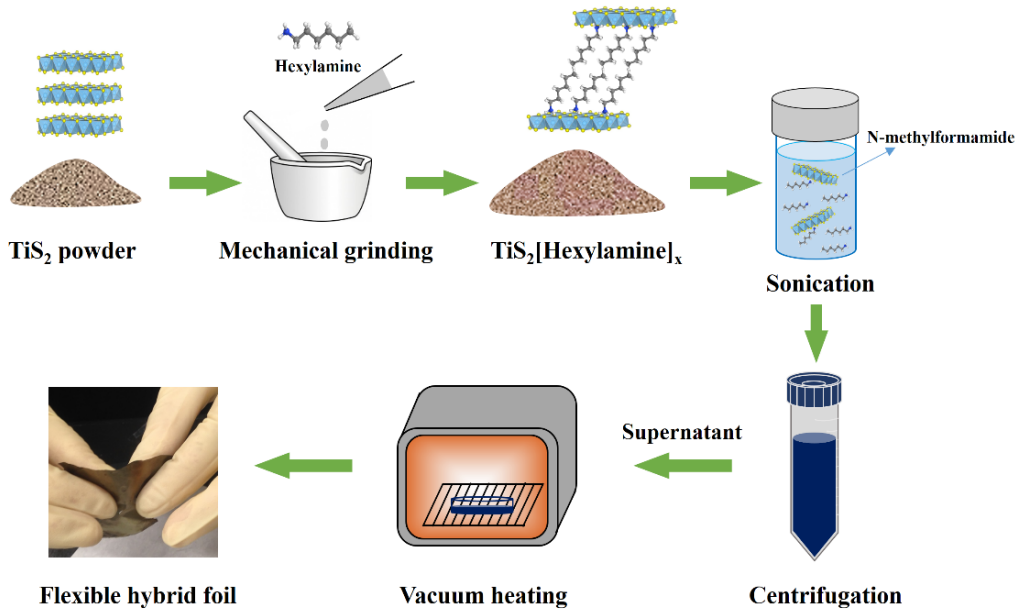

Figure 2

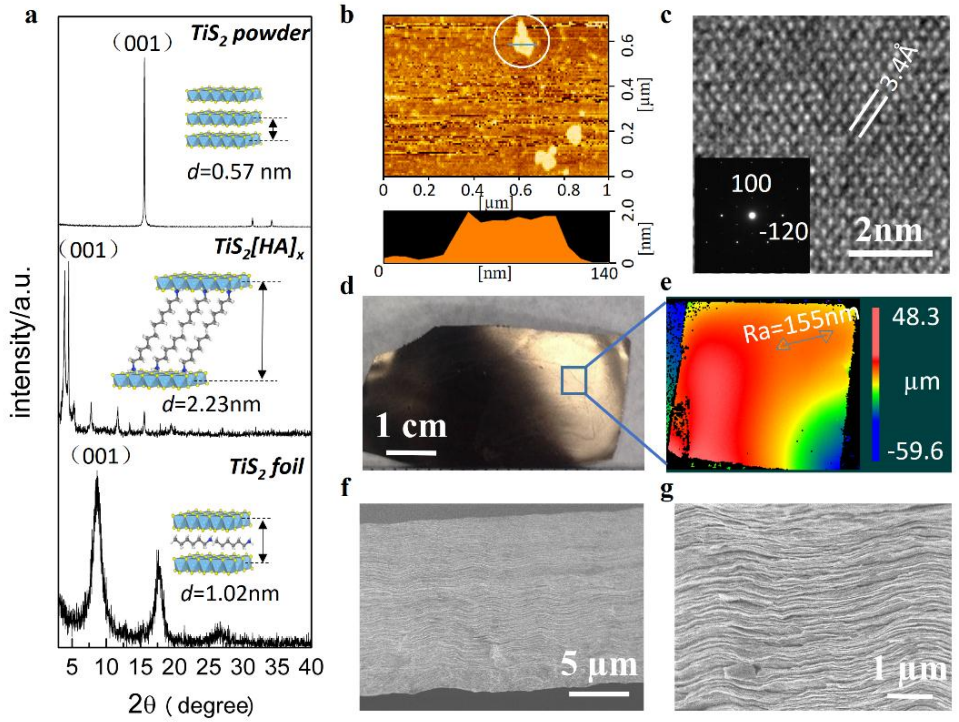
a
(001)
TiS2 powder
d=0.57 nm
(001)
TiS2[HA]x
d=2.23nm
(001)
TiS2 foil
d=1.02nm
intensity/a.u.
5 10 15 20 25 30 35 40
2θ (degree)
b
[μm]
[nm]
c
3.4Å
100
-120
2nm
d
1 cm
e
Ra=155nm
48.3
μm
-59.6
f
5 μm
g
1 μm

Figure 3

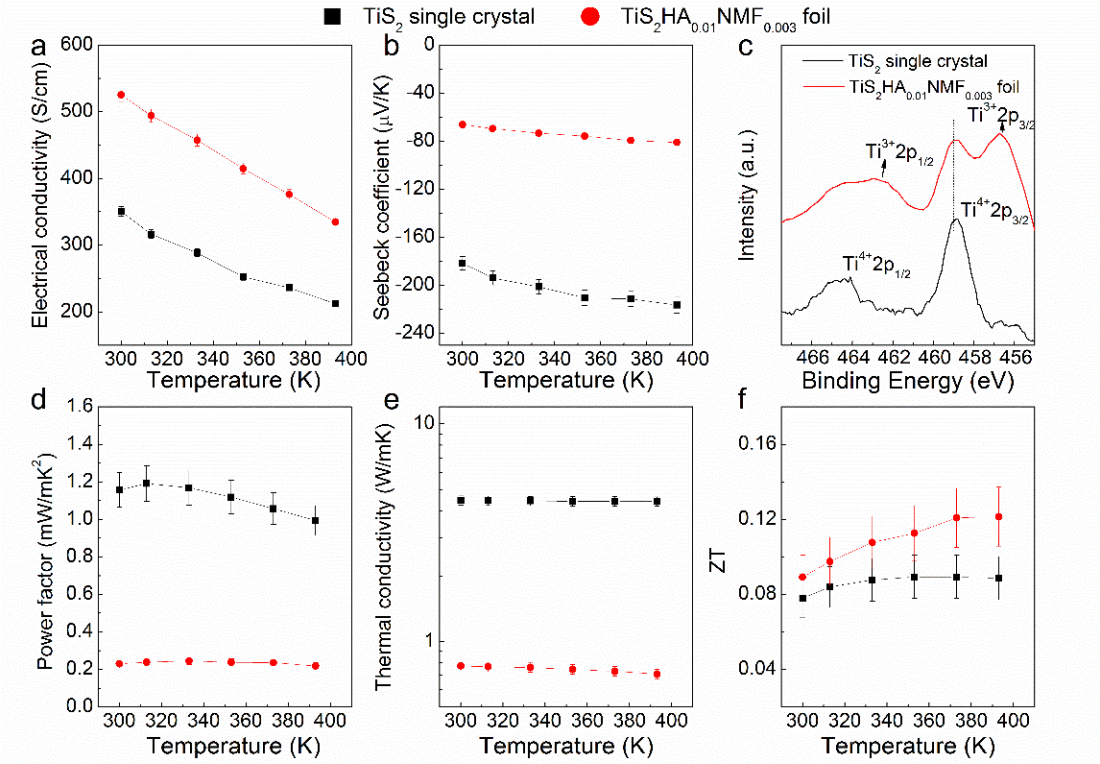
TiS2 single crystal
TiS2HA0.01NMF0.003 foil
a
Electrical conductivity (S/cm)
Temperature (K)
b
Seebeck coefficient (μV/K)
Temperature (K)
c
TiS2 single crystal
TiS2HA0.01NMF0.003 foil
Ti3+2p3/2
Ti3+2p1/2
Ti4+2p3/2
Ti4+2p1/2
Intensity (a.u.)
Binding Energy (eV)
d
Power factor (mW/mK2)
Temperature (K)
e
Thermal conductivity (W/mK)
Temperature (K)
f
ZT
Temperature (K)

Figure 4

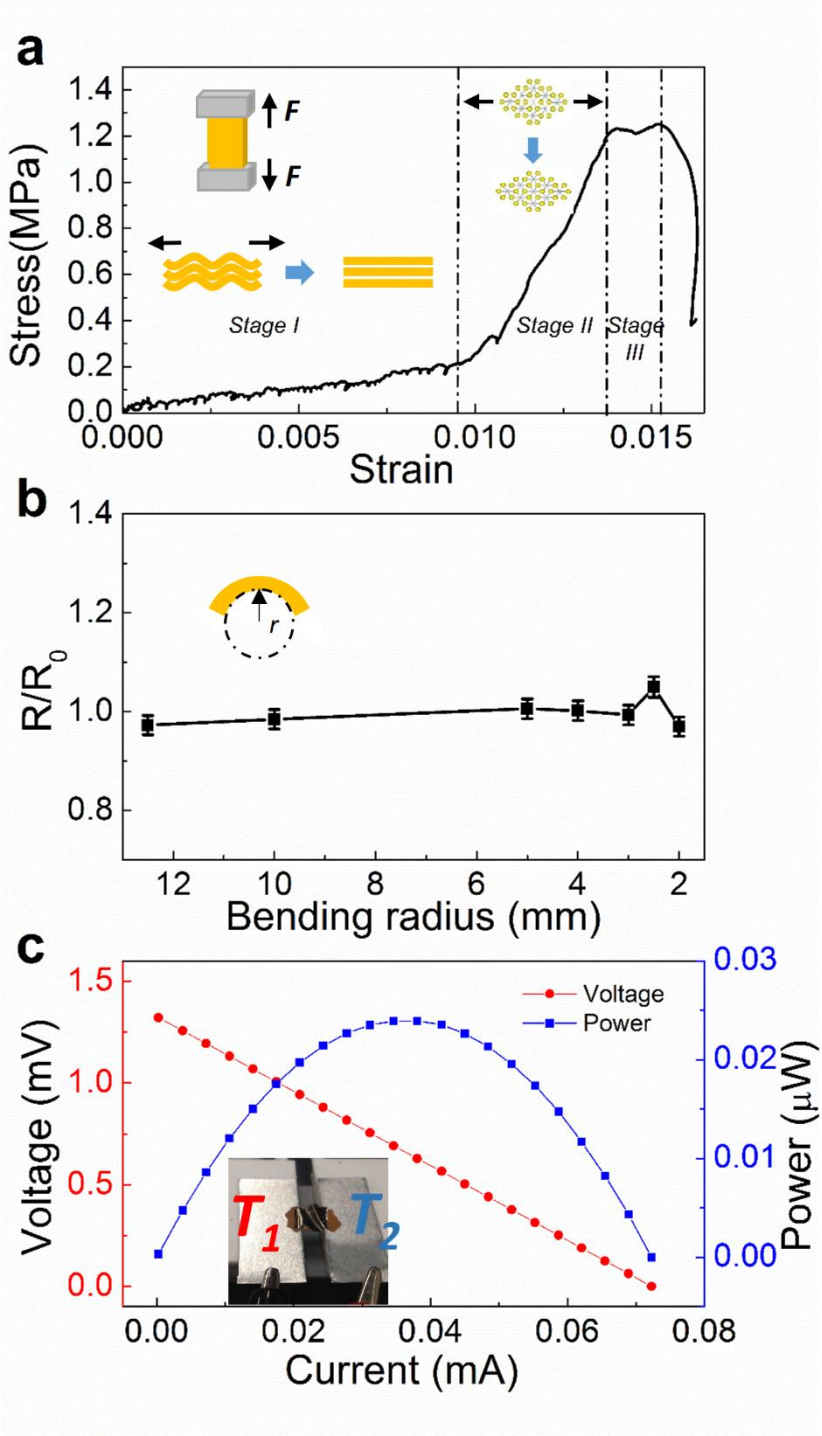

Highlights

Fabrication of freestanding large-area thermoelectric foil with a hybrid inorganic/organic superlattice structure

Demonstration of high power factor and output power in the n-type flexible thermoelectric foil

Demonstration of flexible thermoelectric energy harvesting with superior bending tolerance